Tracing prices: A flow-based cost allocation for optimized power systems

F. Hofmann

October 21, 2020

Abstract

Cost minimization of power systems leads to perfectly scheduled operations and investments while securing all power demands. System needs reports from regional, national and international agencies increasingly rely on cost minimization techniques. However, cost impact to single regions and thefore the question of who profits to what extent from an investment is often neglected. The literature provides multiple cost allocation methods dedicated to this problem, yet they hardly suit for large networks and an integration of all costs. This work introduces a peer-to-peer allocation of all system costs in optimized models. Combining basic relations from economic optimization with flow allocation, its cost assignments locally constraint while still being aligned with the Locational Marginal Prices at the optimum. It is showcased by means of an optimized near-future scenario of the German power system.

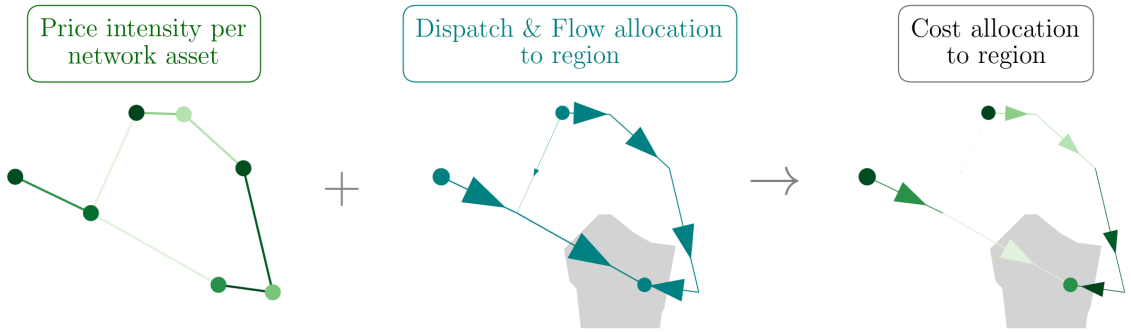

Highlights

- In long-term equilibria a network asset gains back its variable and investment cost from its operation based revenue
- Flow tracing is used as a basis to allocate the operation of assets to consumers.
- Allocated flows have to be reshaped such that the Kirchhoff Current Law and the Kirchhoff Voltage Law are respected.
- Using operational and shadow prices from constraints, all costs are assigned in an P2P manner.
- The cost assignments are locally constraint and in alignment with the nodal pricing scheme.
- In a low-carbon scenario for Germany regions with high renewable potentials profit from investment compensated by remote buses.

Nomenclature

$\lambda_{n,t}$	Locational Market Price at bus n and time step t in €/MW
$d_{n,t}$	Electric demand per bus n, demand type a, time step t in MW
$s_{i,t}$	Operational state of asset i, at time step t in MW
o_i	Operational price of asset i in €/MW
c_i	Capital Price of asset i in €/MW
$K_{n,i}$	Incidence values ($\neq 0$ if i is attached to n)

1 Introduction

Today's power systems are subject to a deep and ongoing transformation. The needed shift to from controllable to weather-driven power generation, the constant improvement and innovation of technology

require rigorous system planning and international cooperation [1, 2]. The core of the problem manifests in the costs. Firstly, these should be as small as possible while meeting ecological and sociological standards. Secondly, they must be distributed in a fair and transparent manner. Cost-driving aspects or market players should be detected and addressed appropriately. In this context, power system modelling has increasingly gained attention during the last years [1, 3, 4]. Many studies show how cost-efficiency and renewable energy are brought together. However, the question of how and, more importantly, upon what grounds costs are distributed was often left open.

This study bridges this gap. On the basis of an optimized network the operational state of each time step and corresponding characteristics are in detailed considered to allocate all system costs. The presented approach builds upon two basic concepts: Firstly, the revenue of an network asset at the cost-optimum exactly matches its operational and capital expenditures, also known as the zero-profit condition. Secondly, flow tracing, following Bialek's Average Participation (AP) [5], can be used to assigns the operation of single network assets to consumers in an plausible and locally constraint manner. Combining these two relations allows for an transparent allocation of all operational (OPEX) and capital expenditures (CAPEX) to the consumers in the network.

Flow-based cost allocation was already discussed and performed in various works [6–12]. Shahidehpour et al. give a deep insight into allocating congestion cost and transmission investments to market participants [7] with different allocation techniques. Based on Generation Shift Factors, *i.e.* the marginal contribution of generators to a flow on line, the Locational Marginal Price (LMP) can be represented as a superposition of LMP at the reference bus, the price for congestion and a price for losses. The approach in [8] expands this relation for contributions based on the AP scheme, which allows for an accurate estimation of the LMP, however does not reflect the exact LMP of an optimized network. A similar approach was taken in [9] where electricity prices of a non-optimal power dispatch were allocated using flow tracing.

The following work brings advantages of all the mentioned studies together. It reassures localized cost allocations while fully aligning payments to the nodal pricing scheme based on the LMP. The work serves to facilitate transparency and cost-benefit analysis in network plannings such as the Ten Year Network Development Plan [13] or the German Netzentwicklungsplan (NEP) [14]. Further, it builds a basis of a usage based transmission cost allocation.

The first section which presents the full method splits into the presentation of: the zero-profit condition for different kind of assets (Section 2.1); the AP allocation scheme and resulting allocation from assets to consumers (Section 2.2); the cost allocation and the impact of additional constraints (Sections 2.3 and 2.4); a numerical example (Section 2.5). The second part in Section 3 applies the cost allocation to a optimized German power system with high shares of renewable power sources and evaluates the allocated costs.

2 Flow-based Cost Allocation

2.1 Zero-Profit Rule

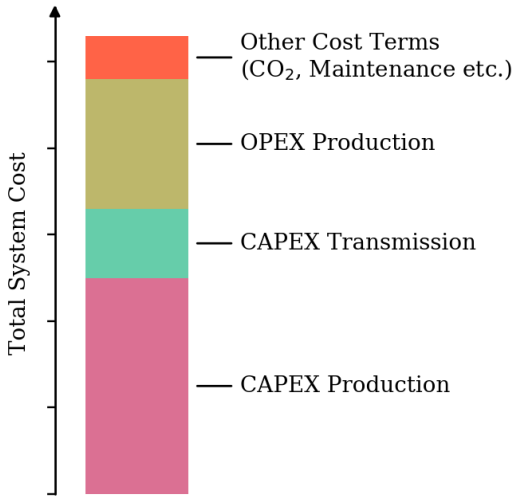

Figure 1: Schematic decomposition of the total system cost $\mathcal{T}$ in an long-term investment model.

In long-term operation and investment planning models, the total costs $\mathcal{T}$ of a power system is the sum of multiple cost terms $\mathcal{C}^\circ$. Typically, these include operational expenditures for generators $\mathcal{O}^G$, expenditures for emissions $\mathcal{E}$, capital investments for the transmission system $\mathcal{I}^F$ and so on, *i.e.*

$$\mathcal{T} = \sum_{\circ} \mathcal{C}^\circ = \mathcal{O}^G + \mathcal{E} + \mathcal{I}^F + \dots \tag{1}$$

In turn, each of the terms $\mathcal{C}^\circ$ consists of the costs

associated to an asset i in the system,

$$\mathcal{C}^\circ = \sum_i \mathcal{C}_i^\circ \tag{2}$$

where an "asset" describes any operating components of the network, such as a generator, line, energy storage etc. We refer to the set of assets as I. In a long-term equilibrium of a power system with perfect competition, the zero-profit condition states that each cost term $\mathcal{C}_i^\circ$ can be considered as a cost-weighted sum of the operational state $s_{i,t}$ of asset i and time t, *i.e.*

$$\mathcal{C}_i^\circ = \sum_t \gamma_{i,t}^\circ \, s_{i,t} \tag{3}$$

where $\gamma_{i,t}^\circ$ denotes a corresponding cost factor in €/MW. If $\mathcal{C}_i^\circ$ describes the OPEX occasioned by asset i, the cost factor $\gamma_{i,t}^\circ$ is simply given by the marginal operational price o_i. However, as we will show in the following, if it describes the CAPEX of asset i, $\gamma_{i,t}^\circ$ is a composition of shadow prices $\mu_{i,t}$ given from the corresponding constraint at the cost-optimum.

For a detailed demonstration, we derive Eq. (3) for generators, transmission lines and storages separately. Therefore, let o_i denote the operational price per MWh of asset i and c_i the capital price for one MW capacity expansion. Table 1 summarizes all derived relations, these can be inserted into Eqs. (2) and (3) for each single cost term.

Generators

Let $S \subseteq I$ be the set of generators in the network, such that $g_{s,t} = s_{s,t}$ describes the power production of generator $s \in S$. The OPEX occasioned by generator s is given by a cost-weighted sum of the production, thus

$$\mathcal{O}_s^G = \sum_t o_s \, g_{s,t} \tag{4a}$$

In case a fix price for emissions μ_{CO2} in € per tonne-CO_2 equivalents, is assumed, a further the cost term per generator s

$$\mathcal{E}_s = \mu_{\mathrm{CO2}} \sum_t e_s \, g_{s,t} \tag{4b}$$

adds to $\mathcal{T}$. Here, e_s denotes the emission factor in tonne-CO_2 per $\mathrm{MWh_{el}}$ of generator s. In contrast to OPEX and emission costs, the CAPEX of S are not a function of the production $g_{s,t}$, but of the actual installed capacity G_s of generator s. In the optimization it limits the generation $g_{s,t}$ in the form of

$$g_{s,t} - G_s \leq 0 \;\perp\; \bar{\mu}_{s,t} \quad \forall\, s,t \tag{4c}$$

The constraint yields a shadow-price of $\bar{\mu}_{s,t}$ in literature often denoted as the Quality of Supply [15]. It can be interpreted as the price per MW that Constr. (4c) imposes to the system. If $\bar{\mu}_{s,t}$ is bigger than zero, the constraint is binding, which pushes investments in G_s. As shown in [16] and in detail in Appendix A.3, over the whole time span, the CAPEX for generator s is payed back by the production $g_{s,t}$ times the shadow price $\bar{\mu}_{s,t}$,

$$\mathcal{I}_s^G = c_s G_s = \sum_t \bar{\mu}_{s,t} \, g_{s,t} \tag{4d}$$

This representation connects the CAPEX with the operational state of generator s, *i.e.* matches the form in Eq. (3).

Transmission Lines

Let $L \subset I$ be the set of transmission lines in the system, these may include Alternating Current (AC) as well as Directed Current (DC) lines. Further let $f_{\ell,t} = s_{\ell,t}$ represent the power flow on line $\ell \in L$. If the OPEX of the transmission system is taken into account in $\mathcal{T}$ (these are often neglected in power system models), these may be approximated by $\mathcal{O}_\ell^F = \sum_t o_\ell |f_{\ell,t}|$, that is, a cost weighted sum of the net flow on line ℓ. Again this stands in contrast to the CAPEX which not a function of $f_{\ell,t}$ but of the transmission capacity F_ℓ. It limits the flow $f_{\ell,t}$ in both directions,

$$f_{\ell,t} - F_\ell \leq 0 \;\perp\; \bar{\mu}_{\ell,t} \quad \forall\, \ell,t \tag{5a}$$

$$-f_{\ell,t} - F_\ell \leq 0 \;\perp\; \underline{\mu}_{\ell,t} \quad \forall\, \ell,t \tag{5b}$$

At the cost-optimum, the two constraints yield the shadow prices $\bar{\mu}_{\ell,t}$ and $\underline{\mu}_{\ell,t}$. We use the relation that over the whole time span, the investment in line ℓ is payed back by the shadow prices times the flow (for details see Appendix A.4)

$$\mathcal{I}_\ell^F = c_\ell F_\ell = \sum_t \left(\bar{\mu}_{\ell,t} - \underline{\mu}_{\ell,t}\right) f_{\ell,t} \tag{5c}$$

Again, the shadow prices $\bar{\mu}_{\ell,t}$ and $\underline{\mu}_{\ell,t}$ can be seen as a measure for necessity of transmission investments

	i	$\mathcal{C}^\circ$	$\mathcal{C}_i^\circ$	$\gamma_{i,t}^\circ$	$s_{i,t}$
OPEX Production	s	$\mathcal{O}^G$	$\sum_t o_s\, g_{s,t}$	o_s	$g_{s,t}$
OPEX Transmission	ℓ	$\mathcal{O}^F$	$\sum_t o_\ell\, \lvert f_{\ell,t}\rvert$	o_ℓ	$\lvert f_{\ell,t}\rvert$
OPEX Storage	r	$\mathcal{O}^E$	$\sum_t o_r\, g_{r,t}^{\text{dis}}$	o_r	$g_{r,t}$
Emission Cost	s	$\mathcal{E}$	$\mu_{\text{CO2}}\, e_s\, g_{s,t}$	$\mu_{\text{CO2}}\, e_s$	$g_{s,t}$
CAPEX Production	s	$\mathcal{I}^G$	$c_s G_s$	$\bar{\mu}_{s,t}$	$g_{s,t}$
CAPEX Transmission	ℓ	$\mathcal{I}^F$	$c_\ell F_\ell$	$\left(\bar{\mu}_{\ell,t} - \underline{\mu}_{\ell,t}\right)$	$f_{\ell,t}$
CAPEX Storage	r	$\mathcal{I}^E$	$c_r G_r$	$\bar{\mu}_{r,t}^{\text{dis}} - \underline{\mu}_{r,t}^{\text{dis}} + (\eta_r^{\text{dis}})^{-1}\lambda_{r,t}^{\text{ene}}$	$g_{r,t}$

Table 1: Mapping of different cost terms to the cost allocation scheme given in Eqs. (8). These include OPEX & CAPEX for production, transmission and storage assets in the network, as well as a cost term for the total Green House Gas (GHG) emissions.

at ℓ at time t. Hence, a non-zero values indicate that Constr. (5a) or (5b) are bound and therefore that the congestion on line ℓ at time t is imposing costs to the system.

Storages

Let $R \in S$ denote all storages in the system. In a simplified storage model, G_r limits the storage dispatch $g_{r,t}^{\text{dis}}$ and charging $g_{r,t}^{\text{sto}}$. Further it limits the maximal storage capacity $g_{r,t}^{\text{ene}}$ by a fix ratio h_r, denoting the maximum hours at full discharge. The storage r dispatches power with efficiency η_r^{dis}, charges power with efficiency η_r^{sto} and preserves power from one time step t to the next, $t+1$, with an efficiency of η_r^{ene}. In Appendix A.5 we formulate the mathematical details. The OPEX term which adds to the objective function is given by

$$\mathcal{O}^E = \sum_r o_r g_{r,t}^{\text{dis}} \tag{6a}$$

Using the result of [16] the CAPEX can be related to the operation of a storage unit r through

$$\begin{aligned}\mathcal{I}^E =& c_r\, G_r \\ =& \sum_t \left(\bar{\mu}_{r,t}^{\text{dis}} - \underline{\mu}_{r,t}^{\text{dis}} + (\eta_r^{\text{dis}})^{-1}\lambda_{r,t}^{\text{ene}}\right) g_{r,t}^{\text{dis}} \\ & - \sum_t \lambda_{n,t} K_{n,r} g_{r,t}^{\text{sto}} \quad \forall\ r\end{aligned} \tag{6b}$$

where $\bar{\mu}_{r,t}^{\text{dis}}$ and $\underline{\mu}_{r,t}^{\text{dis}}$ are the shadow prices of the upper and lower dispatch capacity bound and $\lambda_{r,t}^{\text{ene}}$ is the shadow price of the energy balance constraint. Following the considerations in Appendix A.5 we restrict to the revenue from dispatched power, *i.e.* the first term in Eq. (6b), for the cost allocation.

2.2 Allocation of Power Dispatch

The fact that all asset related costs $\mathcal{C}_i^\circ$ can be represented as a cost-weighted sum of the operational state $s_{i,t}$, prompts the question how the operational state $s_{i,t}$, in turn, is allocated to consumers. This builds the second crucial ingredient of the cost allocation.

Dispatch and flow in a system can be considered as a superposition of individual contributions of nodes and assets. In order to artificially quantify these contribution, the literature provides various methods, named flow allocation schemes. Each of these follow a specific set of assumptions which result in peer-to-peer allocations $A_{m\to n}$. That is a measure for the power supplied at node m and consumed at node n.

In the following, we resort to one specific flow allocation scheme Average Participation (AP), also known as Flow Tracing. The basic idea is to trace the power injection at bus m through the network while following the real power flow on transmission lines and applying the principal of proportional sharing. At each bus, including the starting bus m, the traced flow might be mixed with incoming power flows from other buses. As soon as the power is absorbed or flowing out of a bus, the traced flow originating from m splits in the same proportion as the total flow. This assumption leads to regionally confined allocation $A_{m\to n}$ based on a straightforward principal. A mathematical formulation of the AP scheme is documented in Appendix B. For a detailed comparison with other scheme we refer to [].

The peer-to-peer allocations $A_{m\to n,t}$ fulfill some basic properties. On the one hand it allocates the all power productions at time t, *i.e.* when summing over all receiving nodes n the allocations yield the gross

power generation of producing assets $i \in S \cup R$ (generators and storages) attached to m, denoted by $g_{m,t}$. Mathematically this translates to

$$g_{m,t} = \sum_{i \in S \cup R} K_{m,i}\, s_{i,t} = \sum_{n} A_{m \to n,t} \tag{7a}$$

where $K_{m,i}$ is 1 if asset i is attached to bus m and zero otherwise. On the other hand, when summing over all supplying nodes, the allocation $A_{m \to n,t}$ yields the gross nodal demand $d_{n,t}$ at node n and time t, which leaves us with

$$d_{n,t} = \sum_{m} A_{m \to n,t} \tag{7b}$$

As the standard formulation implies, we assume that only net power production of m is allocated to other buses. That is, if the nodal generation $g_{m,t}$ does not exceed the nodal demand $d_{m,t}$, all of it is allocated to local consumers, *i.e.* $A_{m \to m,t} = \min(g_{m,t}, d_{m,t})$. The principal of proportional sharing sets the allocation of a single producing asset $i \in S \cup R$ proportional to the nodal allocation $A_{m \to n,t}$ and weights it by the share $w_{i,t} = K_{m,i} s_{i,t} / g_{m,t}$ that asset i contributes to the nodal generation $g_{m,t}$, leading to

$$A_{i,n,t} = w_{i,t} A_{m \to n,t} \quad \forall\, i \in S \cup R, n, t \tag{7c}$$

This relation builds one crucial key to the cost allocation. It states how much of the power produced by asset $i \in S \cup R$ is finally consumed by consumers at n.

Yet, we didn't touch the allocation of transporting assets $i \in L$ to consumers. Note that the traced flow based in the AP scheme does obey the Kirchhoff Current Law but not the Kirchhoff Voltage Law, as already pointed out in [6]. However, as we show later a consideration of both laws is needed in order to align the allocated costs with the optimized Locational Marginal Prices. To tackle this, let $H_{\ell,n}$ denote a linear mapping between the injection $(g_{m,t} - d_{m,t})$ and the flow $f_{\ell,t}$, such that

$$f_{\ell,t} = \sum_{m} H_{\ell,m}\, (g_{m,t} - d_{m,t}) \quad \forall\, \ell \in L, t \tag{7d}$$

Usually, $H_{\ell,n}$ is given by the Power Transfer Distribution Factors (PTDF) which indicate the changes in the flow on line ℓ for one unit (typically one MW) of net power production at bus m. For transport models or networks with High Voltage Directed Current (HVDC) lines, these can retrospectively be calculated or extended using the formulation presented in [17]. Inserting Eq. (7a) into Eq. (7d) and expanding the sum yields

$$A_{\ell,n,t} = \sum_{m} H_{\ell,m}\, (A_{m \to n,t} - \delta_{nm} d_{n,t}) \quad \forall\, \ell \in L, n, t \tag{7e}$$

Complementary to Eq. (7c), this allocation indicates the power flow on line ℓ and time t which is finally consumed by $d_{n,t}$.

With Eqs. (7c) and (7e) a full set of allocations between the operational state $s_{i,t}$ of asset $i \in I$ is derived. Naturally, the sum over all receiving nodes reproduces the operational state $s_{i,t}$ of asset i,

$$s_{i,t} = \sum_{n} A_{i,n,t} \quad \forall\, i, t \tag{7f}$$

2.3 Cost Allocation

Using the presented relations, we are able to straightforwardly define the full cost allocation. Therefore, the expanded sum in Eq. (7f) is inserted in Eq. (3) which leads to

$$\mathcal{C}^{\circ}_{n \to i,t} = \gamma^{\circ}_{i,t}\, A_{i,n,t} \tag{8a}$$

By default, all cost of a cost term $\mathcal{C}^{\circ}_{i}$ associated with asset i are allocated, thus $\mathcal{C}^{\circ}_{i} = \sum_{n} \mathcal{C}^{\circ}_{n \to i,t}$; likewise all system costs are distributed, $\mathcal{T} = \sum_{\circ,i,n,t} \mathcal{C}^{\circ}_{n \to i,t}$.

The cost allocation entails a further important property. In a cost-optimal setup with minimized $\mathcal{T}$, the Locational Marginal Price (LMP) describes the change of costs for an incremental increase of electricity demand $d_{n,t}$ at node n and time t [15]. Mathematically this translates to the derivative of the total system cost $\mathcal{T}$ with respect to the local demand $d_{n,t}$, $\lambda_{n,t} = \partial \mathcal{T} / \partial d_{n,t}$. At the optimum this quantity is given by a shadow price of the nodal balance constraint (see Appendix A.1 for details). Now, when summing over all assets i and cost terms $\circ$, the cost allocation yields

$$\mathcal{C}_{n,t} = \sum_{\circ,i} \mathcal{C}^{\circ}_{n \to i,t} = \lambda_{n,t}\, d_{n,t} \quad \forall\, n, t \tag{8b}$$

which we refer to as the nodal payment or payment. It exactly matches the payment determined by the LMP $\lambda_{n,t}$. Hence, Equation (8b) which is in detailed proved in Appendix A.6 shows that the cost allocation is embedded in the nodal pricing scheme implied by the LMP.

2.4 Design Constraints

Power system modelling does rarely follow a pure Greenfield approach with unlimited capacity expansion. Rather, today's models are setting various constraints defining socio-political or technical requirements. However, this will alter the equality of total cost and total revenue. More precisely, each constraint h_j (other then the nodal balance constraint) of the form

$$h_j\left(s_{i,t}, S_i\right) < K \tag{9a}$$

where K is any non-zero constant and S_i denotes the nominal capacities of asset i, will alter Eq. (3) to

$$\mathcal{C}_i^\circ - \mathcal{R}_i^\circ = \sum_t \gamma_{i,t}^\circ \, s_{i,t} \tag{9b}$$

$$= \sum_{n,t} \mathcal{C}_{n\to i,t}^\circ \tag{9c}$$

According to the nature of Eq. (9a) and the corresponding $\mathcal{R}_i$, it is either larger, equal or lower than $\mathcal{C}^\circ$. Whereas Eq. (8b) still holds true, the total of payments do not return the total system cost $\mathcal{T}$ anymore. The total mismatch $\mathcal{R}$ is given by

$$\mathcal{R} = \mathcal{T} - \sum_{n,t} \mathcal{C}_{n,t} \tag{9d}$$

In the following we highlight two often used classes of designs constraints in the form of Eq. (9a) and show how to consider them into the cost allocation.

Capacity Expansion Limit

In real-world setups, generators, lines or other assets can often only be built up to a certain limit. This might be due to land use restrictions or social acceptance considerations. When constraining the capacity S_i to an upper limit $\bar{S}$, in the form of

$$S_i - \bar{S} \leq 0 \;\perp\; \bar{\mu}_i^{\text{nom}} \quad \forall\, i \in I, \tag{10a}$$

the zero profit condition alters as soon as the constraint becomes binding. Then, asset i is payed an additional scarcity rent

$$\mathcal{R}_i^{\text{scarcity}} = -\bar{\mu}_i^{\text{nom}} S_i \quad \forall\, i \in I \tag{10b}$$

This rent may account for different possible realms, as for example the increased market price due in higher competed areas or additional costs for social or environmental compensation. To end this, the share in $\mathcal{C}_{n\to i,t}^\circ$ which consumers pay for the scarcity rent can be recalculated by a correct weighting the shadow price $\bar{\mu}_s^{\text{nom}}$ with the capital price c_i, leading to

$$\mathcal{R}_{n\to i,t}^{\text{scarcity}} = \frac{\bar{\mu}_i^{\text{nom}}}{c_i + \bar{\mu}_i^{\text{nom}}} \mathcal{C}_{n\to i,t}^\circ \quad \forall\, i \tag{10c}$$

Brownfield Constraints

In order to take already built infrastructure into account, the capacity S_i can be constrained to a minimum required capacity $\underline{S}$. This introduces a constraint of the form

$$\underline{S} - S_i \leq 0 \;\perp\; \underline{\mu}_i^{\text{nom}} \quad \forall i \in I \tag{11a}$$

Again, such a setup alters the zero profit condition of asset i, as soon as the constraint becomes binding. In that case, asset i does not collect enough revenue from $\mathcal{C}_{n\to i,t}^\circ$ in order to match the CAPEX. The difference, given by

$$\mathcal{R}_i^{\text{subsidy}} = \underline{\mu}_i^{\text{nom}} S_i \quad \forall\, i \tag{11b}$$

has to be subsidized by governments or communities or is simply ignored when investments are amortized. Note, it is rather futile wanting to allocate these cost to consumers as assets may not gain any revenue for their operational state, *i.e.* where $\mathcal{C}^\circ = \mathcal{R}_i^{\text{subsidy}}$.

2.5 Numerical Example

Consider a two bus system, depicted in Fig. 2, with one transmission line and one generator per bus. Generator 1 (at bus 1) has a cheap operational price of 50 €/MWh_{el}, generator 2 (at bus 2) has a expensive operational price of 200 €/MWh_{el}. For both, capital investments amount 500 €/MW and the maximal capacity is limited to $\bar{G}_s = 100$ MW. The transmission line has a capital price of 100 €/MW and no upper capacity limit. With a demand of 60 MW at bus 1 and 90 MW at bus 2, the optimization expands the cheaper generator at bus 1 to its full limit of 100 MW. The 40 MW excess power, not consumed at bus 1, flows to bus 2 where the generator is built with only 50 MW.

Figure 3 shows the allocation $A_{i,n,t}$ for $n = 1$ and $n = 2$ separately. The "sum" of the two figures give to the actual dispatch and flow. The resulting P2P payments are given in Fig. 4.

The left graph Fig. 3a shows that d_1 is with 60 MW totally supplied by the local production.

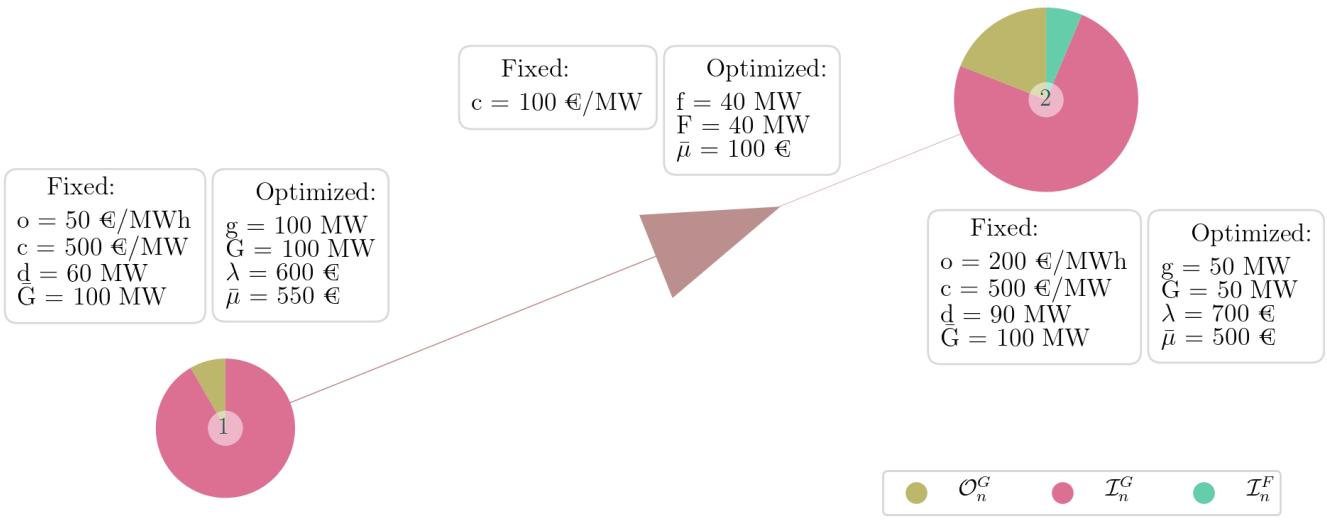

Figure 2: Illustrative example of a 2 bus network with one optimized time step. Fixed prices and constraining values are given in the left box for each bus and the transmission line. Optimized values are given in the right boxes. Generator 1 at bus 1 has a cheaper operational price o, capital prices are the same for both. As both generator capacities are constraint to 100 MW, the optimization also deploys the generator at bus 2.

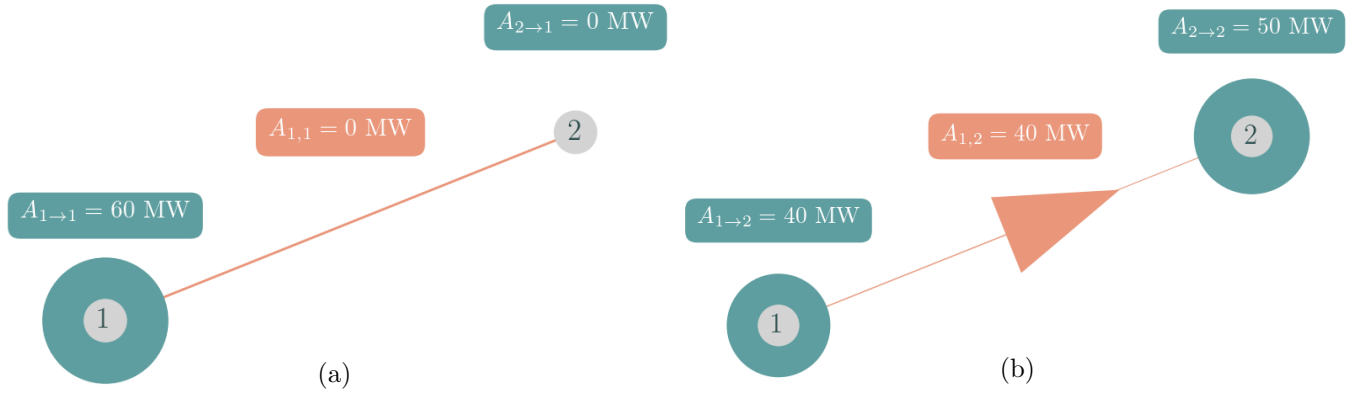

Figure 3: Power allocations $A_{i,n,t}$ in the example network Fig. 2 using Average Participation. Consumers at for bus 1, figure (a), are, with 60 MW, totally supplied by the local generator and do not consume any imported power from bus 2. In contrast consumer at bus 2, figure (b), retrieve 40 MW from generator 1, induce a flow of 40 MW on the transmission line and consume 50 MW from the local generator.

Consequently consumers at bus 1 pay 3k € OPEX, which is the operational price of 50 € times the 60 MW. Further they pay 33k € for the CAPEX at generator 1. Note that 3k € of these account for the scarcity imposed buy the upper expansion limit $\bar{G}_s$. The rest makes up 60% of the total CAPEX spent at generator 1, exactly the share of power allocated to d_1. Consumers at bus 1 don't pay any transmission CAPEX as no flow is associated with there demand. The right graph Fig. 3b shows the power allocations to d_2. We see that 50 MW are self-supplied whereas the remaining 40 MW are imported from generator 1. Thus, consumers pay for the local OPEX and CAPEX as well as the proportional share of expenditures at bus 1 and the transmission system. As the capacity at generator 2 does not hit the expansion limit $\bar{G}_s$, no scarcity cost are assigned to it. The allocated $\mathcal{I}^G_{2\to2}$ compensates the full investment of generator 2. Again, 2k€ of the 22k€ which are allocated to investment in generator 1 are associated with the scarcity cost for generator 1. The payed congestion revenue of 4k€ is exactly the CAPEX of the transmission line. The sum of all values in the payoff matrix in Fig. 4 yield $\mathcal{T} - \mathcal{R}^{\text{scarcity}}$, the

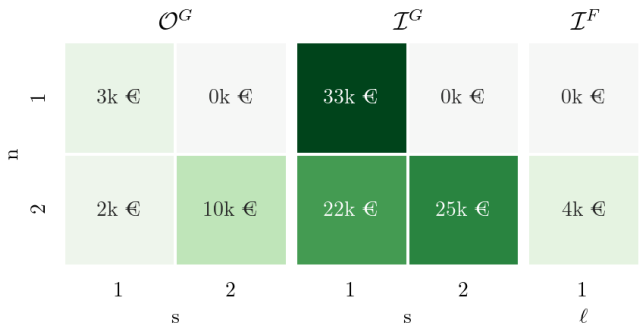

Figure 4: Full P2P cost allocation $\mathcal{C}^{\circ}_{n\to i,t}$ on the optimized example network in Fig. 2. Consumers compensate OPEX and CAPEX of the generators they retrieve from (compare with Fig. 3). As bus 1 is totally self-supplying, all it payment is assigned to the local generator. As bus 2 imports power from bus 1 and thus induces a flow on line 1, it not only compensates local expenditures but also OPEX and CAPEX at bus 1 and CAPEX for the transmission.

total system cost minus the scarcity cost (which in turn is negative). The sum of a column yields the total revenue per the asset i. These values match their overall spending plus the cost of scarcity. The sum a row returns the nodal payments $C_n = \lambda_n\, d_n$. For example the sum of payments of consumers at bus 1 is 36k€ . This is exactly the electricity price of 600 €/MW times the consumption of 60 MW, $\lambda_1 d_1$.

The fact that OPEX and CAPEX allocations are proportional to each other results from optimizing one time step only. This coherence breaks for larger optimization problems with multiple time steps. Then CAPEX allocation takes effect only for time steps in which one or more of the capacity constraints Constrs. (4c), (5a) and (5b) become binding.

3 Application Case

We showcase the behavior of the cost allocation in a more complex system, by applying it to an cost-optimized German power system model with 50 nodes and one year time span with hourly resolution. The model builds up on the PyPSA-EUR workflow [18] with technical details and assumptions reported in [19].

We follow a brownfield approach where transmission lines can be expanded starting from today's capacity values, originally retrieved from the ENTSO-E Transmission System Map [20]. Pre-installed wind and solar generation capacity totals of the year 2017 were distributed in proportion to the average power potential at each site excluding those with an average capacity factor of 10%. Further, wind and solar capacity expansion are limited by land use restriction. These consider agriculture, urban, forested and protected areas based on the CORINE and NATURA2000 database [21, 22]. Pumped Hydro Storages (PHS) and Run-of-River power plants are fixed to today's capacities with no more expansion allowed. Additionally, unlimited expansion of batteries and H_2-storages and Open-Cycle Gas Turbines (OCGT) are allowed at each node. We impose a effective carbon price of 120 € per tonne-CO_2 which, for OCGT, adds an effective price of 55 €/MWh_{el}(assuming a gross emission of 180 kg/MWh and an efficiency of 39%). All cost assumptions on operational costs o_i and annualized capital cost c_i are summarized in detail in Table 2.

The optimized network is shown in Fig. 5. On the left we find the lower capacity bounds for renewable generators and transmission infrastructure, on the right the capacity expansion for generation, storage and transmission are displayed. The optimization expands solar capacities in the south, onshore and offshore wind in the upper north and most west. Open-Cycle Gas Turbines (OCGT) are build within the broad middle of the network. Transmission lines are amplified in along the north-south axis, including one large DC link, associated with the German Süd-Link, leading from the coastal region to the southwest. The total annualized cost of the power system roughly sums up to 42 billion €.

Figure 6 displays the load-weighted average electricity price $\bar{\lambda}_n$ per region, defined by

$$\bar{\lambda}_n = \frac{\sum_t \lambda_{n,t} d_{n,t}}{\sum_t d_{n,t}} \tag{12}$$

We observe a relatively strong gradient from south (at roughly 92 €/MWh) to north (80 €/MWh). Regions with little pre-installed capacity and capacity expansion, especially with respect to renewable generation, tend to have higher prices. The node with the lowest LMP in the upper northwest, stands out through high pre-installed offshore capacities.

In Fig. 7 we show the total of all allocated costs.

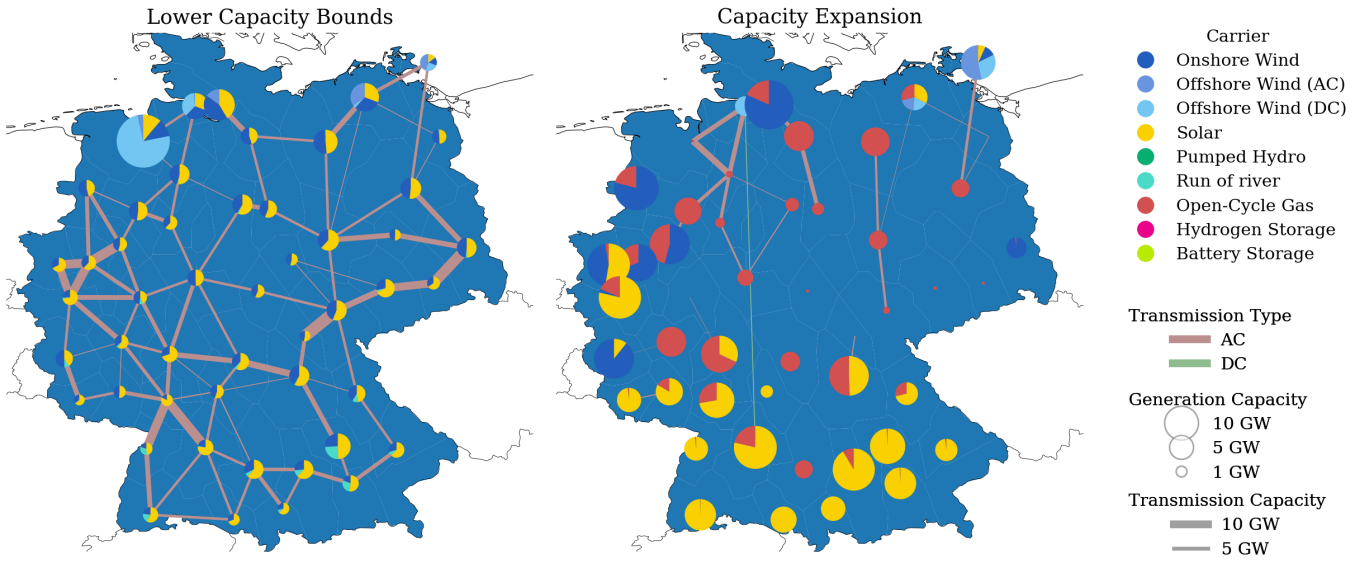

Figure 5: Brownfield optimization of the German power system. The left side shows existent renewable capacities, matching the total capacity for the year 2017, which serve as lower capacity limits for the optimization. The right side shows the capacity expansion of renewable resources as well as installation of backup gas power plants. The effective CO_2 price is set to 120 €per tonne CO_2 emission.

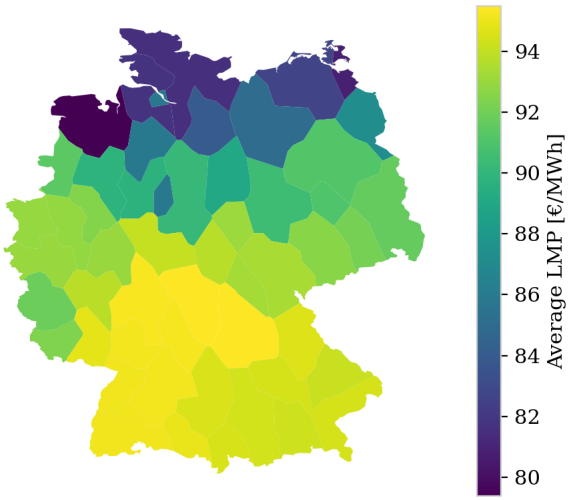

Figure 6: Average electricity price $\bar{\lambda}_n$ per region as a result from the optimization of the German power system. Regions in the middle and south of Germany have high prices whereas electricity in the North with a strong wind, transmission and OCGT infrastructure is cheaper.

The allocated cost to capital expenditures is given by $\mathcal{C}^\circ - \mathcal{R}^\circ$. The difference $\mathcal{R}$ consists of scarcity rents $\mathcal{R}^{\text{scarcity}}$ and subsidies $\mathcal{R}^{\text{subsidy}}$. Note that the sum of all contributions in Fig. 7 equals the total cost $\mathcal{T}$. In the following, we address each of the displayed cost terms and its corresponding allocations separately.

The largest proportion of the payments is associated with CAPEX for generators, transmission system and storage units in decreasing order. Taking different technologies into account, we observe a fundamental difference between the controllable OCGT and the variable renewable resources: As shown in detail in Fig. C.6, more than half of all investments in OCGT is determined in one specific hour. At this time (morning, end of February), the system hits the highest mismatch between low renewable power potentials and high demands. The necessity for backup generators manifests in high allocation of CAPEX for OCGT and consequently high LMP. With a few exceptions in the South West and East, all consumers receive power from OCGT at this time, thus all pay high amounts for the needed backup infrastructure (operational state of the system is in detailed shown in Fig. C.7). Note that this is the most extreme event, which ensures backup infrastructure for other inferior extreme events. The total CAPEX allocation for OCGT infrastructure is depicted in Fig. C.1d. This

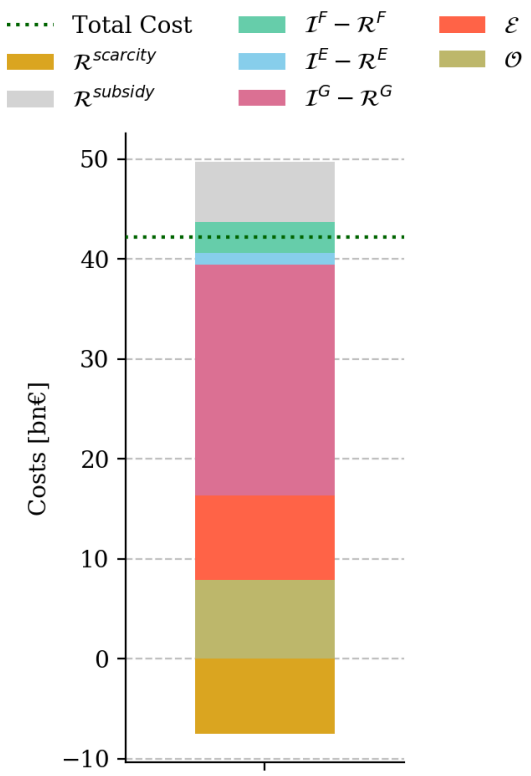

Figure 7: Total allocated payments of the system.

correlates with our findings of the extreme event. Contrary to this, CAPEX for renewable infrastructure are allocated evenly throughout several thousands of hours. As for onshore and offshore wind farms, the produced power deeply penetrates the network, see Fig. C.4, thus it is not only local, but also remote consumers which cover the CAPEX, see Fig. C.1. This in turn benefits local consumers, which profit from the cheap operational prices of local wind farms. This explains why these regions end up with a low average LMP.

Together with the emission cost $\mathcal{E}$, the total OPEX $\mathcal{O}$ amount around 16 billion €. As to expect, 99.97% are dedicated to OCGT alone, as these have by far the highest operational price. For a detailed regional distribution of payments per MWh and the resulting revenues for generator, see Figs. C.2 and C.3. Since during ordinary demand peaks, it is rather local OCGT generators which serve as backup generators, thus the OPEX allocation of OCGT clearly differs from the CAPEX allocation. In the average power mix per region, see Fig. C.4, we observe that regions with strong OCGT capacities predominately have high shares of OCGT power. The average operational price for renewable generators is extremely low (0.2 €/MWh), thus they play an inferior role in the OPEX allocation.

The negative segment in Fig. 7 is associated with scarcity costs $\mathcal{R}^{\text{scarcity}}$, caused by land use constraints for renewable resources and the transmission expansion limit. These sum up approximately to 7.5 b€. Note again, that according to Eq. (10b) this term is negative and is part of the allocated CAPEX payments. It translates to the cost that consumers pay "too much" for assets limited in their capacity expansion. In the real world this money would be spent for augmented land costs or civic participation in the dedicated areas. In Fig. C.9 we give a detailed insight of how the scarcity cost manifest in the average cost per consumed MWh. The scarcity for wind and solar is relatively low and impact the average price at roughly 2€/MWh. It primarily affects, different to the pure CAPEX allocation, regions in close vicinity. Remarkably, the scarcity cost per MWh for run-of-river power plants amounts up to 16€. This high impact is due to the steady power potential from run-off water and the strong limitation of capacity expansion. However, as these power plants in particular are already amortized, the scarcity cost should be reconsidered and removed from a final cost allocation.

A high influence on the price comes from the scarcity of transmission expansion. Right beside regions with high wind infrastructure, it occasions costs higher than MWh 4€/MWh (maximal 8€/MWh), see Fig. C.8. As to expect, the constraint mainly suppresses transmission expansion along the north-south axis.

The last cost term in Fig. 7, is caused by lower capacity constraints for pre-existing assets. These violate the optimal design and are not compensated through the nodal payments $d_{n,t}\,\lambda_{n,t}$. Most of these "non-allocatable" costs account for Pumped Hydro Storage, onshore wind, offshore wind and the transmission system, see Fig. C.5 for further details. Again, as most of the named assets are already amortized (PHS, transmission system), the subsidy should be reconsidered in a final cost allocation.

In Fig. 8 we compare the total cost allocation of the region with the lowest average LMP (left side) against the one of the region with the highest LMP (right side). The region with the cheapest electricity is in

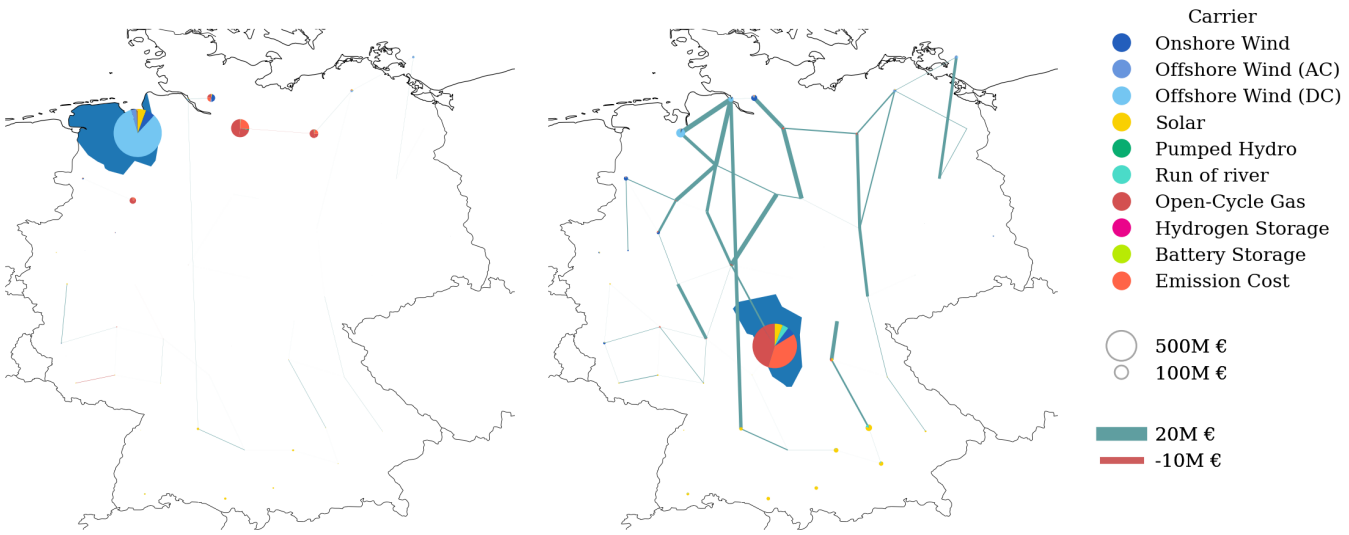

Figure 8: Comparison of payments of the node with the **lowest LMP (left)** and the node with the **highest LMP (right)**. The region of the paying bus is colored in dark blue. The circles indicate where to which bus and technology combined OPEX and CAPEX payments. Further the thickness of the lines indicates the dedicated amount of payments. The cheap prices in the North...

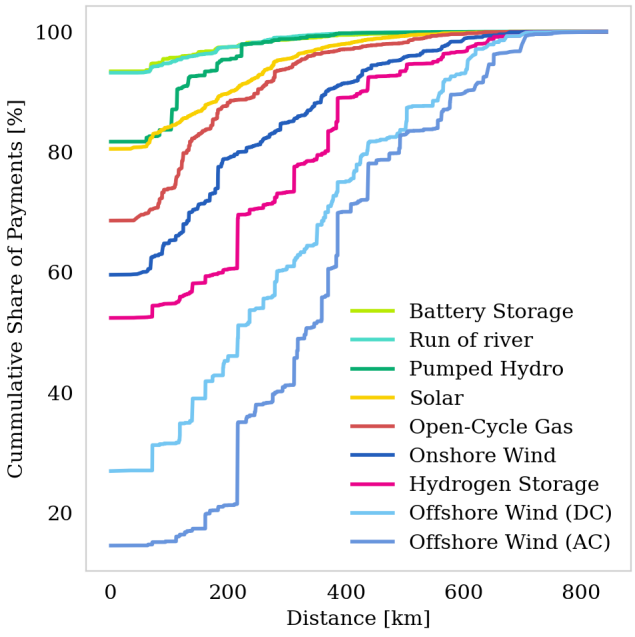

Figure 9: Average distance between payer and receiver for different technologies and shares of the total production.

the Northwest. We see that this bus is fairly independent of investments in the transmission system, as it is supplied by steady, cheap offshore power. Moreover, the CAPEX of the local offshore wind farms are partly payed by subsidies, see Fig. C.5. Only a small share of the payments is allocated to remote OCGTs, resulting from the extreme event mentioned earlier.

In contrast the regions with the highest LMP, spends most its money to local OCGT operations, emission cost and the transmission system. Its payments to onshore and offshore wind infrastructure are low despite a third of its supply comes from wind power. Instead, a lot of its payments are assigned to the transmission infrastructure. Hence, the wind power supply at this region is not restricted by exhausted wind power resources but by bottlenecks in the transmission system.

4 Limitations

The presented cost allocation is based on the linear power flow approximation. Yet, the method is equally applicable to a system with an Optimal Power Flow (OPF), *i.e.* full AC power flows. However, the AP scheme might not the right choice as the Kirchhoff Voltage Law cannot not be considered subsequently as done here. Rather, the Z-Bus flow al-

location presented in [23] might be a better choice as it considers by default the two circuit laws. Allocating on the basis of the full power flow introduces an additional cost term $\mathcal{R}^{\text{Loss}}$ accounting for the transmission loss which is compensated by the consumers and mirrors in the LMP.

The used optimization does not consider security constrains of the transmission system, this can however be incorporated by introducing by following security constrained optimal power flow (SCOPF) as done in [10].

In the presented work, we restricted the application to long term investment models with perfect foresight. However, the cost allocation can as well be applied to short term planning models with fixed capacities. The revenue from the capacity limits then builds basis for amortization and future investments.

The optimization assumed a fix demand time series. As shown in Fig. C.6 this leads to high if not unrealistic LMP. Introducing a value of loss load as proposed in [24] would screen away these and lead to more evenly distributed allocations.

5 Conclusion and Outlook

A new cost-allocation scheme based on peer-to-peer dispatch allocations from assets to consumers was presented. Within a long-term equilibrium OPEX and CAPEX of each asset are payed back by the operation based revenue. Using flow allocation, we are able to allocate the operation and therefore the assigned costs of assets to consumers in the network. For three typical classes of assets, namely generators, transmission lines and storage units, we showed how operational prices and shadow prices must be weighted with the dispatch allocation in order to allocate all system costs. Further we highlighted the impact of minimum capacity requirements and maximum installation potentials. These alter the revenues per asset and therefore the cost allocations. For lower capacity requirements, the cost have to be subsidized by the overall system operator or the government, as those cannot be allocated. Contrary, upper capacity expansion limits lead to an additional charge for consumers which have to compensate for *e.g.* land use restrictions. Applied to a optimized German power system with an imposed price of 120 € per tonne CO_2 equivalent, the cost allocation shows how buses remote from wind farms pay higher prices due to increased reliance in transmission and backup capacity. On the other hand, buses with high renewable installation spend most payments to local assets.

Reproducibility

All figures and number of the plot can be reproduced by using the *snakemake* workflow in [].

Funding

This research was funded by the by the German Federal Ministry for Economics Affairs and Energy in the frame of the NetAllok project [25].

Acknowledgement

Special thanks to Tom Brown for fruitful discussions and well-placed inputs.

A Network Optimization

A.1 LMP from Optimization

The nodal balance constraint ensures that the amount of power that flows into a bus equals the power that flows out of a bus, thus reflects the Kirchhoff Current Law (KCL). Alternatively, we can the demand $d_{n,t}$ has to be supplied by the attached assets,

$$g_{n,t} - \sum_{\ell} K_{n,\ell} f_{\ell,t} = d_{n,t} \;\perp\; \lambda_{n,t} \quad \forall\, n,t \tag{A.1}$$

where $K_{n,\ell}$ is +1 if line ℓ starts at bus n, -1 if it ends at n, 0 otherwise. The nodal generation $g_{n,t}$ collects all nodal production, see Eq. (7a). The shadow price of the nodal balance constraint mirrors the Locational Marginal Prizes (LMP) $\lambda_{n,t}$ per bus and time step. In a power market this is the €/$\mathrm{MWh_{el}}$-price which a consumer has to pay.

A.2 Full Lagrangian

The Lagrangian for the investment model can be condensed to the following expression

$$\begin{aligned}\mathcal{L}\left(s_{i,t}, S_i, \lambda_{n,t}, \mu_j\right) = \\ &+ \sum_{i,t} o_i s_{i,t} + \sum_{i} c_i S_i \\ &+ \sum_{n,t} \lambda_{n,t} \left(d_{n,t} - g_{n,t} + \sum_{\ell} K_{n,\ell}\, f_{\ell,t} \right) \\ &+ \sum_{j} \mu_j\, h_j\left(s_{i,t}, S_i\right)\end{aligned} \tag{A.2}$$

where $h_j\left(s_{i,t}, S_i\right)$ denotes all inequality constraints attached to $s_{i,t}$ and S_i. Note that according to Eq. (7a) $g_{n,t}$ is a composition of $s_{i,t}$ and $f_{\ell,t} = s_{\ell,t} \forall \ell \in L$.

In order to impose the Kirchhoff Voltage Law (KVL) for the linearized AC flow, the term

$$\sum_{\ell,c,t} \lambda_{c,t}\, C_{\ell,c}\, x_\ell\, f_{\ell,t} \tag{A.3}$$

can be added to $\mathcal{L}$, with x_ℓ denoting the line's impedance and $C_{\ell,c}$ being 1 if ℓ is part of the cycle c and zero otherwise.

The global maximum of the Lagrangian requires stationarity with respect to all variables:

$$\frac{\partial \mathcal{L}}{\partial s_{i,t}} = \frac{\partial \mathcal{L}}{\partial S_i} = 0 \tag{A.4}$$

A.3 Zero Profit Generation

For each generator the optimization defines a lower capacity constraint, given by

$$-g_{s,t} \le 0 \;\perp\; \underline{\mu}_{s,t} \quad \forall\, s,t \tag{A.5}$$

Constrs. (4c) and (A.5), which yield the KKT variables $\bar{\mu}_{s,t}$ and $\underline{\mu}_{s,t}$, imply the complementary slackness,

$$\bar{\mu}_{s,t}\left(g_{s,t} - \bar{g}_{s,t}\, G_s\right) = 0 \quad \forall\, s,t \tag{A.6}$$

$$\underline{\mu}_{s,t}\, g_{s,t} = 0 \quad \forall\, s,t \tag{A.7}$$

The stationarity of the generation capacity variable leads to

$$\frac{\partial \mathcal{L}}{\partial G_s} = 0 \;\rightarrow\; c_s = \sum_{t} \bar{\mu}_{s,t}\, \bar{g}_{s,t} \quad \forall\, s \tag{A.8}$$

and the stationarity of the generation to

$$\frac{\partial \mathcal{L}}{\partial g_{s,t}} = 0 \;\rightarrow\; o_s = \sum_{n} K_{n,s}\, \lambda_{n,t} - \bar{\mu}_{s,t} + \underline{\mu}_{s,t} \quad \forall\, s \tag{A.9}$$

Multiplying both sides of Eq. (A.8) with G_s and using Eq. (A.6) leads to

$$c_s\, G_s = \sum_{t} \bar{\mu}_{s,t}\, g_{s,t} \quad \forall\, s \tag{A.10}$$

The zero-profit rule for generators is obtained by multiplying Eq. (A.9) with $g_{s,t}$ and using Eqs. (A.7) and (A.10) which results in

$$c_s\, G_s + \sum_{t} o_s g_{s,t} = \sum_{n,t} \lambda_{n,t} K_{n,s} g_{s,t} \quad \forall\, s \tag{A.11}$$

It states that over the whole time span, all OPEX and CAPEX for generator s (left hand side) are payed back by its revenue (right hand side).

A.4 Zero Profit Transmission System

The yielding KKT variables $\bar{\mu}_{\ell,t}$ and $\underline{\mu}_{\ell,t}$ are only non-zero if $f_{\ell,t}$ is limited by the transmission capacity in positive or negative direction, i.e. Constr. (5a) or

Constr. (5b) are binding. For flows below the thermal limit, the complementary slackness

$$\bar{\mu}_{\ell,t}\,(f_{\ell,t} - F_\ell) = 0 \quad \forall\ \ell, t \tag{A.12}$$
$$\underline{\mu}_{\ell,t}\,(f_{\ell,t} - F_\ell) = 0 \quad \forall\ \ell, t \tag{A.13}$$

sets the respective KKT to zero.

The stationarity of the transmission capacity to

$$\frac{\partial \mathcal{L}}{\partial F_\ell} = 0 \ \rightarrow\ c_\ell = \sum_t \left(\bar{\mu}_{\ell,t} - \underline{\mu}_{\ell,t}\right) \quad \forall\ \ell \tag{A.14}$$

and the stationarity with respect to the flow to

$$0 = \frac{\partial \mathcal{L}}{\partial f_{\ell,t}} \tag{A.15}$$
$$0 = -\sum_n K_{n,\ell}\lambda_{n,t} + \sum_c \lambda_{c,t} C_{\ell,c} x_\ell - \bar{\mu}_{\ell,t} + \underline{\mu}_{\ell,t} \quad \forall\ \ell, t \tag{A.16}$$

When multiplying Eq. (A.14) with F_ℓ and using the complementary slackness Eqs. (A.12) and (A.13) we obtain

$$c_\ell\, F_\ell = \sum_t \left(\bar{\mu}_{\ell,t} - \underline{\mu}_{\ell,t}\right)\, f_{\ell,t} \quad \forall\ \ell \tag{A.17}$$

Again we can use this to formulate the zero-profit rule for transmission lines. We multiply Eq. (A.16) with $f_{\ell,t}$, which finally leads us to

$$c_\ell\, F_\ell = -\sum_n K_{n,\ell}\,\lambda_{n,t}\, f_{\ell,t} + \sum_c \lambda_{c,t}\, C_{\ell,c}\, x_\ell\, f_{\ell,t} \quad \forall\ \ell \tag{A.18}$$

It states that the congestion revenue of a line (first term right hand side) reduced by the cost for cycle constraint exactly matches its CAPEX.

A.5 Zero Profit Storage Units

For an simplified storage model, the upper capacity G_r limits the discharging dispatch $g^{\text{dis}}_{r,t}$, the storing power $g^{\text{sto}}_{r,t}$ and state of charge $g^{\text{ene}}_{r,t}$ of a storage unit r by

$$g^{\text{dis}}_{r,t} - G_r \le 0 \ \perp\ \bar{\mu}^{\text{dis}}_{r,t} \quad \forall\ r, t \tag{A.19}$$
$$g^{\text{sto}}_{r,t} - G_r \le 0 \ \perp\ \bar{\mu}^{\text{sto}}_{r,t} \quad \forall\ r, t \tag{A.20}$$
$$g^{\text{ene}}_{r,t} - h_r\, G_r \le 0 \ \perp\ \bar{\mu}^{\text{ene}}_{r,t} \quad \forall\ r, t \tag{A.21}$$

where we assume a fixed ratio between dispatch and storage capacity of h_r. The state of charge must be consistent throughout every time step according to what is dispatched and stored,

$$g^{\text{ene}}_{r,t} - \eta^{\text{ene}}_r g^{\text{ene}}_{r,t-1} - \eta^{\text{sto}}_r g^{\text{sto}}_{r,t} + (\eta^{\text{dis}}_r)^{-1} g^{\text{dis}}_{r,t} = 0 \ \perp\ \lambda^{\text{ene}}_{r,t} \quad \forall\ r, t \tag{A.22}$$

We use the result of Appendix B.3 in [16] which shows that a storage recovers its capital (and operational) costs from aligning dispatch and charging to the LMP, thus

$$\sum_t o_r\, g^{\text{dis}}_{r,t} + c_r\, G_r = \sum_t \lambda_{n,t} K_{n,r} \left(g^{\text{dis}}_{r,t} - g^{\text{sto}}_{r,t}\right) \quad \forall\ r, t$$

The stationarity of the dispatched power leads us to

$$\frac{\partial \mathcal{L}}{\partial g^{\text{dis}}_{r,t}} = 0$$
$$o_r - \sum_n \lambda_{n,t}\, K_{n,r} - \underline{\mu}^{\text{dis}}_{r,t} + \bar{\mu}^{\text{dis}}_{r,t} + (\eta^{\text{dis}}_r)^{-1} \lambda^{\text{ene}}_{r,t} = 0\ \forall r, t \tag{A.23}$$

which we can use to define the revenue which compensates the CAPEX at r,

$$c_r\, G_r = \sum_t \left(\bar{\mu}^{\text{dis}}_{r,t} - \underline{\mu}^{\text{dis}}_{r,t} + (\eta^{\text{dis}}_r)^{-1} \lambda^{\text{ene}}_{r,t}\right) g^{\text{dis}}_{r,t} - \sum_t \lambda_{n,t} K_{n,r} g^{\text{sto}}_{r,t} \quad \forall\ r \tag{A.24}$$

When applying the cost allocation scheme Eqs. (8), it stands to reason to assume that when a storage charges power, it does not supply any demand. Thus consumers only pay storage units in times the storage dispatches power. Hence, we restrict the allocatable revenue per storage unit to the first term in Eqs. (6b) and (A.24). This allocates then the CAPEX of r plus the costs $\mathcal{R}^E_r$ it needs to buy the charging power,

$$\mathcal{I}^E_r + \mathcal{R}^E_r = \sum_t \left(\bar{\mu}^{\text{dis}}_{r,t} - \underline{\mu}^{\text{dis}}_{r,t} + (\eta^{\text{dis}}_r)^{-1} \lambda^{\text{ene}}_{r,t}\right) g^{\text{dis}}_{r,t} \tag{A.25}$$

In charging times the total of remaining costs $\mathcal{R}^E_r$ is spent to power from other assets. These costs scale with the amount of installed storage capacity. Note that it would be possible to incorporate this redistribution into the cost allocation, by replacing the demand $d_{n,t}$ with the power charge $g^{\text{sto}}_{r,t}$ in Eqs. (8). Then, the derived payments that a storage unit r has to pay to asset i is given by $\mathcal{C}^\circ_{r\to i}$. The sum of those payments due to r will the sum up to $\mathcal{R}^E_r$.

A.6 Proof: Equivalence of local and imported prices

We start with Eq. (A.16) which we recall here,

$$0 = -\sum_m K_{m,\ell}\lambda_{m,t} + \sum_c \lambda_{c,t} C_{\ell,c} x_\ell - \bar{\mu}_{\ell,t} + \underline{\mu}_{\ell,t} \quad \forall\, \ell, t \tag{A.26}$$

It states that the price difference between two adjacent buses minus the price for the KVL, is the revenue per line ℓ, $\left(-\bar{\mu}_{\ell,t} + \underline{\mu}_{\ell,t}\right)$. We multiply the equation by the flow allocation $A_{\ell,n,t}$ and obtain

$$\begin{aligned} 0 = &- A_{\ell,n,t} \sum_m K_{m,\ell}\lambda_{m,t} \\ &+ A_{\ell,n,t} \sum_c \lambda_{c,t} C_{\ell,c} x_\ell \\ &- A_{\ell,n,t} \left(\bar{\mu}_{\ell,t} - \underline{\mu}_{\ell,t}\right) \quad \forall\, \ell, t \end{aligned} \tag{A.27}$$

The allocation $A_{\ell,n,t}$ defined in Eq. (7e)follows the linear power flow laws. We slightly reformulate the expression to

$$A_{\ell,n,t} = \sum_{m'} H_{\ell,m'} \left(A_{m'\to n,t} - \delta_{nm'} d_{n,t}\right) \quad \forall\, \ell, n, t \tag{A.28}$$

and insert it into Eq. (A.27). When taking the sum over all lines L, the first term yields

$$\begin{aligned} &- \sum_{\ell,m'} H_{\ell,m'} \left(A_{m'\to n,t} - \delta_{nm'} d_{n,t}\right) \sum_m K_{m,\ell}\lambda_{m,t} \\ &= - \sum_{\ell,m',m} H_{\ell,m'} \left(A_{m'\to n,t} - \delta_{nm'} d_{n,t}\right) K_{m,\ell}\lambda_{m,t} \\ &= - \sum_{m',m} \delta_{mm'} \left(A_{m'\to n,t} - \delta_{nm'} d_{n,t}\right) \lambda_{m,t} \\ &= - \sum_m \left(A_{m\to n,t} - \delta_{nm} d_{n,t}\right) \lambda_{m,t} \\ &= - \sum_m A_{m\to n,t}\lambda_{m,t} + d_{n,t}\lambda_{n,t} \end{aligned} \tag{A.29}$$

where in the third step we used the relation $\sum_\ell H_{\ell,n} K_{m,\ell} = \delta_{nm}$. The second term in Eq. (A.27) vanishes as the basis cycles $C_{\ell,c}$ are the kernel of the PTDF, $\sum_\ell C_{\ell,c} H_{\ell,n} = 0\ \forall c, n$. Thus, we end up with

$$\begin{aligned} d_{n,t}\lambda_{n,t} = &\sum_m A_{m\to n,t}\lambda_{m,t} \\ &+ \sum_\ell A_{\ell,n,t} \left(\bar{\mu}_{\ell,t} - \underline{\mu}_{\ell,t}\right) \quad \forall\, n, t \end{aligned} \tag{A.30}$$

This relation shows that for any P2P allocations $A_{m\to n,t}$ the combined price of the imported power is always be the same as the locational price. The representation matches the findings in [12]. However, the latter builds its formulation on a evenly distributed slack, which translated to a peer-to-peer allocation $A_{m\to n,t}$ corresponding to the non-local Equivalent Bilateral Exchanges [6]. However, the representation here holds only true any $A_{m\to n,t}$ if the corresponding flow allocation $A_{\ell,n,t}$ follow the power flow laws, *i.e.* are defined as in Eqs. (7e) and (A.28).

Naturally, the power production of the supplying node m decomposes into contributions of assets, following the definition in Eq. (7c). At the same time, the LMP at m decomposes into asset related prices (Eqs. (A.9) and (A.23)). This finally reproduces the allocations of Table 1 and results in

$$d_{n,t}\,\lambda_{n,t} = \sum_{\circ,i} \mathcal{C}^{\circ}_{n\to i,t} \tag{A.31}$$

B Power Allocation

Allocating net injections using the AP method is derived from [26]. In a lossless network the downstream and upstream formulations result in the same P2P allocation which is why we restrict ourselves to the downstream formulation only. In a first step we define a time-dependent auxiliary matrix $\mathcal{J}_t$ which is the inverse of the $N \times N$ with directed power flow $m \to n$ at entry (m, n) for $m \neq n$ and the total flow passing node m at entry (m, m) at time step t. Mathematically this translates to

$$\mathcal{J}_t = \left(\operatorname{diag}\left(p^+\right) + \mathcal{K}^- \operatorname{diag}\left(f\right) K\right)^{-1}_t \tag{B.32}$$

where $\mathcal{K}^-$ is the negative part of the directed Incidence matrix $\mathcal{K}_{n,\ell} = \operatorname{sign}\left(f_\ell\right) K_{n,\ell}$. Then the P2P allocation for time step t is given by

$$A_{m\to n,t} = \mathcal{J}_{m,n,t}\, p^+_{m,t}\, p^-_{n,t} \tag{B.33}$$

C Working Example

The following figures contain more detailed information about the peer-to-peer cost allocation. The cost or prices payed by consumers are indicated by the region color. The dedicated revenue is displayed in proportion to the size of cycles (for assets attached to buses) or to the thickness of transmission branches.

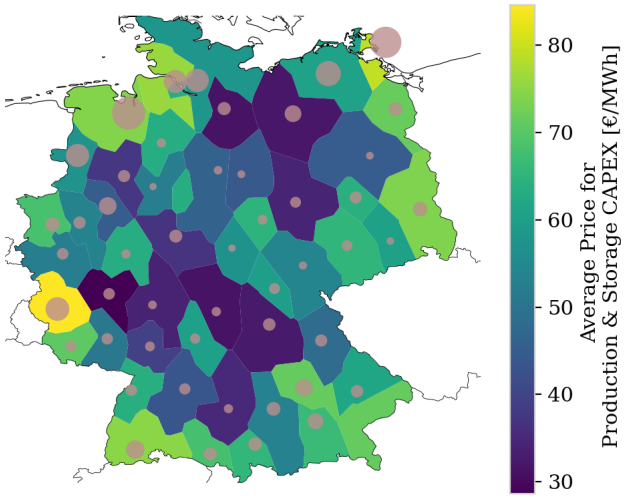

(a) All production and storage technologies

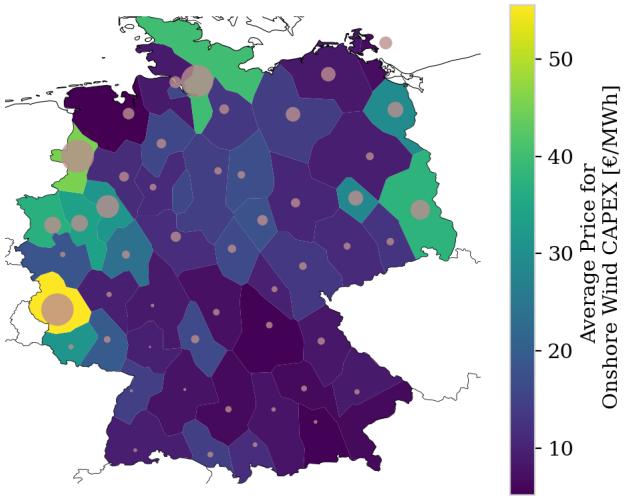

(b) Onshore Wind

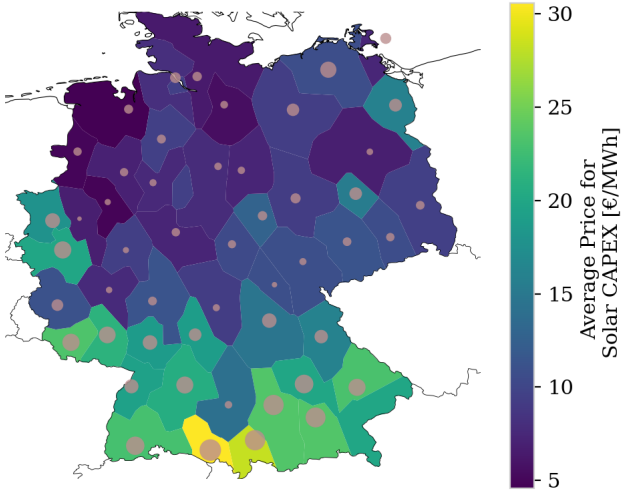

(c) Solar

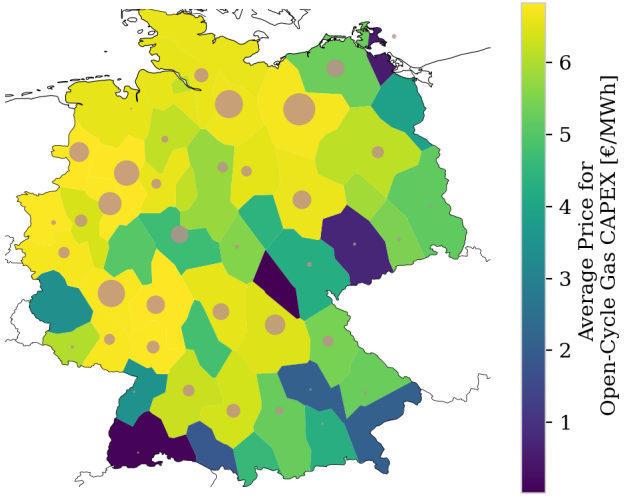

(d) OCGT

Figure C.1: Average **CAPEX allocation** per MWh, $\sum_t \mathcal{I}^G_{n\to s,t} / \sum_t d_{n,t}$ and $\sum_t \mathcal{I}^E_{n\to r,t} / \sum_t d_{n,t}$, for all production and storage assets (a), onshore wind (b), solar (c) and OCGT (d). Average Allocated CAPEX per MWh within the regions are indicated by the color, the revenue per production asset is given by the size of the circles at the corresponding bus.

	carrier	o [€/MWh]	c [k€/MW]*
Generator	Open-Cycle Gas	120.718	47.235
	Offshore Wind (AC)	0.015	204.689
	Offshore Wind (DC)	0.015	230.532
	Onshore Wind	0.015	109.296
	Run of river		270.941
	Solar	0.01	55.064
Storage	Hydrogen Storage		224.739
	Pumped Hydro		160.627
	Battery Storage		133.775
Line	AC		0.038
	DC		0.070

Table 2: Operational and capital price assumptions for all type of assets used in the working example. The capital price for transmission lines are given in [k€/MW/km]. The cost assumptions are retrieved from the PyPSA-EUR model [18].

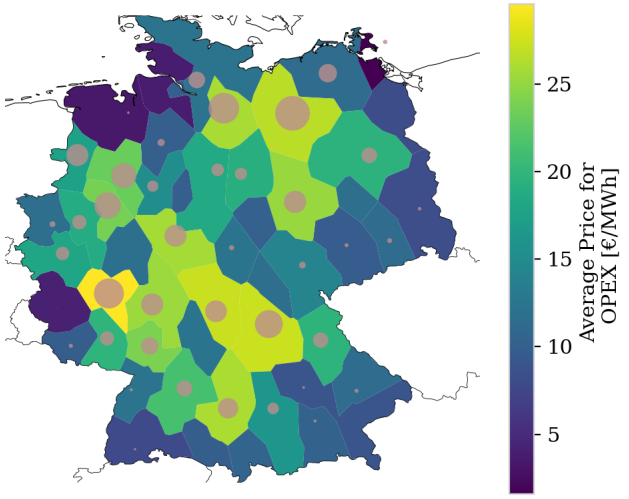

Figure C.2: Average **OPEX allocation** per consumed MWh, $\sum_t \mathcal{O}_{n\to s,t} / \sum_t d_{n,t}$. The effective prices for OPEX are indicated by the color of the region, the size of the circles are set proportional to the revenue per regional generators and storages. As OCGT is the only allowed fossil based technology, the drawn allocation is proportional to OPEX allocation of OCGT generators.

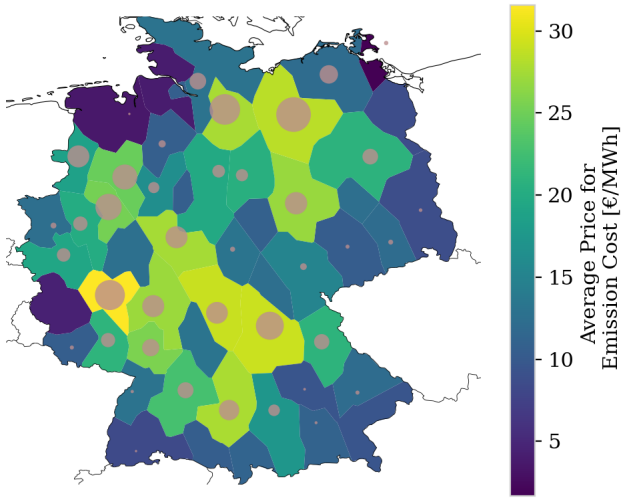

Figure C.3: Average **allocated emission cost**, $\sum_t \mathcal{E}_{n\to s,t}$, per consumed MWh. The effective prices are indicated by the color of the region, the size of the circles are set proportional to the revenue per regional generators.

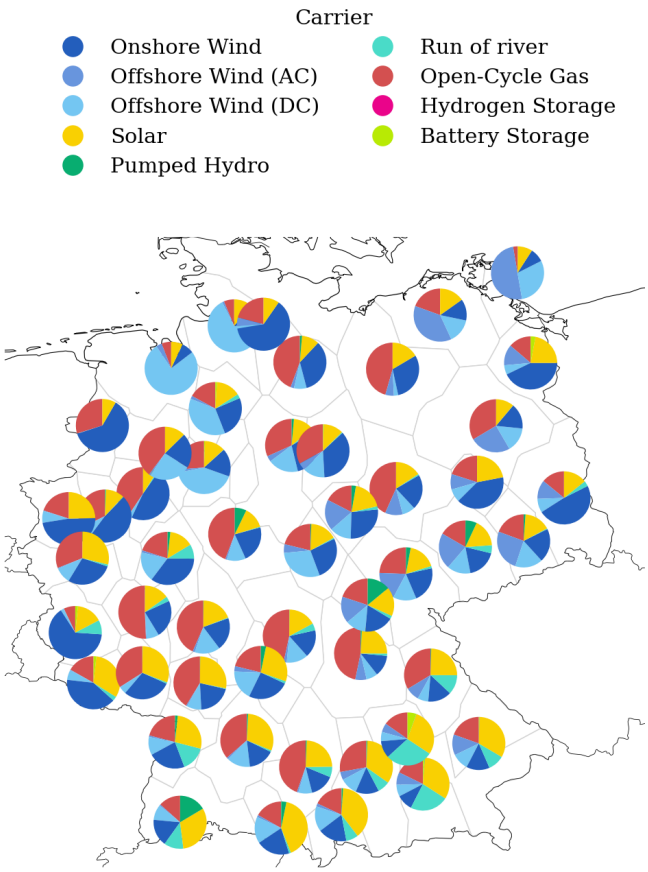

Figure C.4: Average power mix per region calculated by Average Participation. Coastal regions are mainly supplied by local offshore and onshore wind farms. Their strong power injections additionally penetrate the network up to the southern border. In the middle and South, the supply is dominated by a combination of OCGT and solar power.

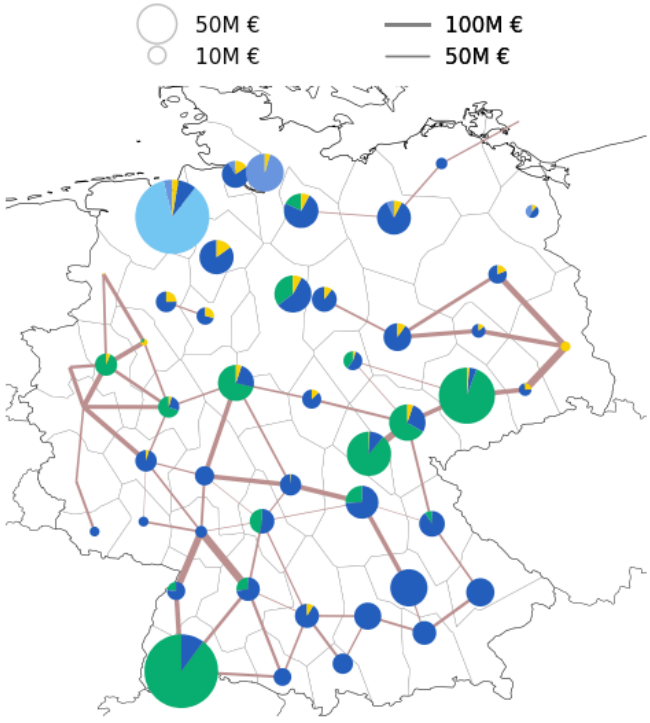

Figure C.5: Total costs for subsidy $\mathcal{R}^{\text{subsidy}}$ resulting from lower capacity expansion bounds (brownfield constraints). The figure shows the built infrastructure that does not gain back its CAPEX from its market revenue, but is only build due to lower capacity limits.

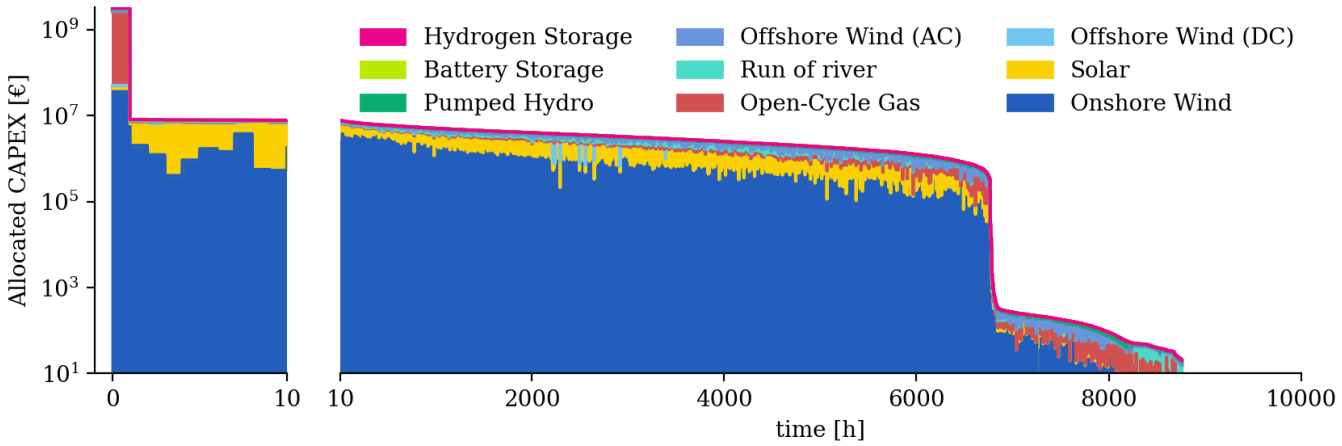

Figure C.6: Duration curve of the CAPEX allocation for production and storage technologies. Hours are sorted by the total amount of allocated expenditure. With 2.7 bn € the first value pushes investments extraordinarily high. Due to low renewable potentials, it is dominated by CAPEX for OCGT which receives 92% of the payments. This hour alone occasions about the half of all OCGT CAPEX. Figure C.6 gives a detailed picture of the operational state at this time-step. The following 7000 time-steps are dominated by revenues for onshore wind and reveal a rather even distribution. In hours of low CAPEX allocation (after the second drop) spending for OCGT start to increase again. These time-steps however play a minor role.

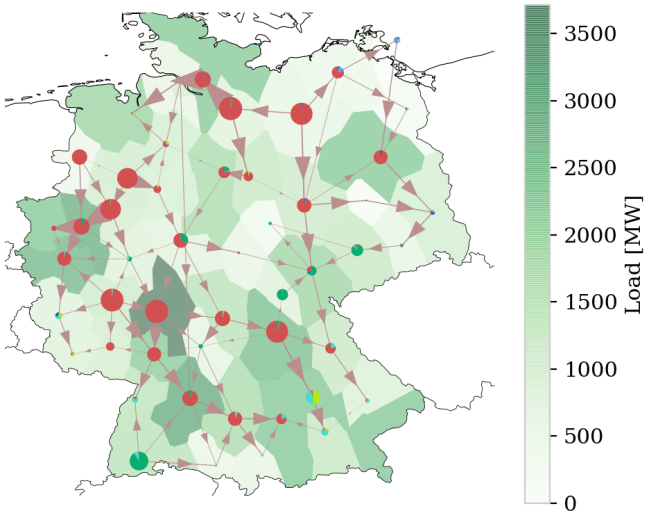

Figure C.7: Production, flow and consumption in the system at the hour with the highest allocated expenditures. The size of the circles are proportional to the power production at a node. Size of arrows are proportional to the flow on the transmission line. The depicted hour corresponds to the first value in the duration curve in Fig. C.6.

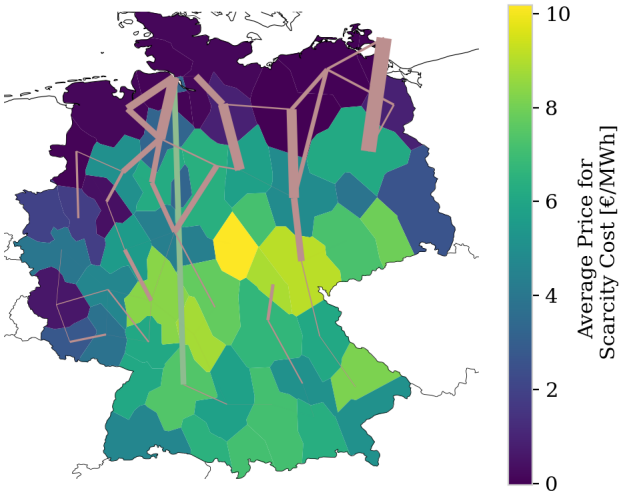

Figure C.8: Average **allocated transmission scarcity cost** per consumed MWh, $\sum_t \mathcal{R}^{\text{scarcity}}_{n\to\ell,t} / \sum_t d_{n,t}$. This scarcity cost results from the upper transmission expansion limit of 25%. The costs are indicated by the regional color. The lines are drawn in proportion to revenue dedicated to scarcity cost.

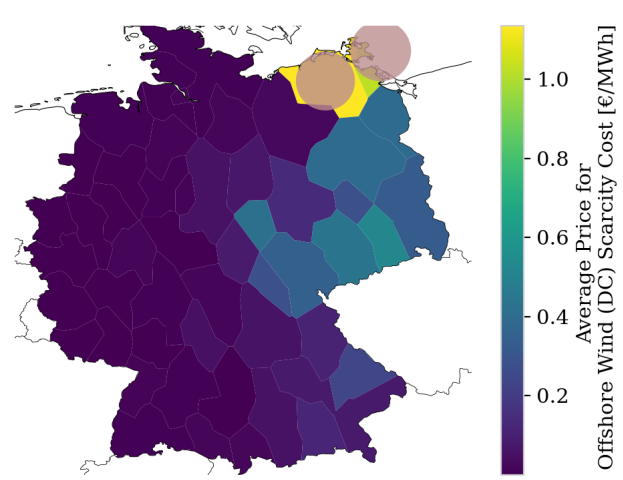

(a) Offshore Wind

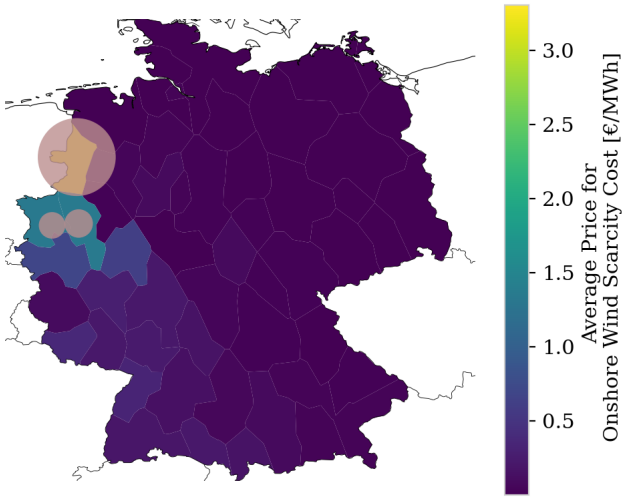

(b) Onshore Wind

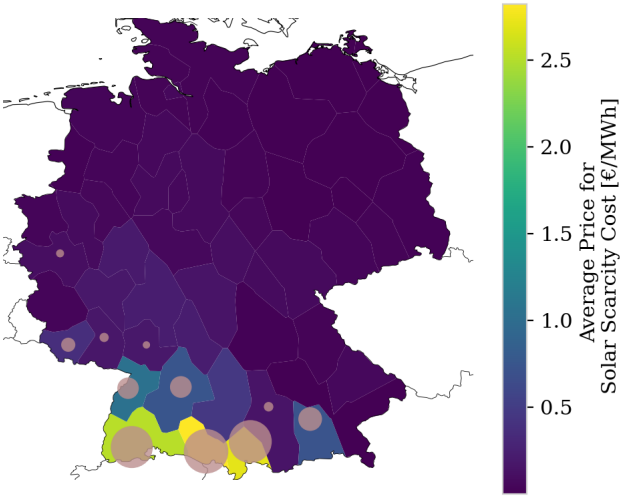

(c) Solar

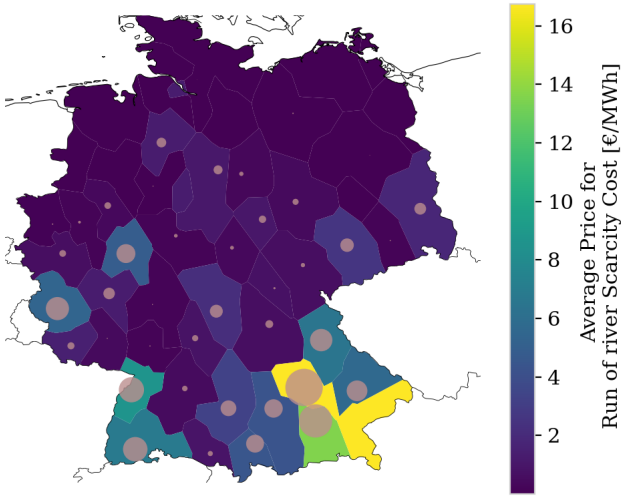

(d) Run-of-River

Figure C.9: Average **allocated scarcity cost** per consumed MWh, $\sum_t \mathcal{R}^{\text{scarcity}}_{n\to i,t} / \sum_t d_{n,t}$. These cost result from land use restrictions for offshore wind, onshore wind, solar, run-of-river. The cost per MWh are indicated by the color of a region. The revenue per production asset is given by the size of the circle at the corresponding bus.

References

[1] Stefan Pfenninger, Adam Hawkes, and James Keirstead. "Energy Systems Modeling for Twenty-First Century Energy Challenges". en. In: *Renewable and Sustainable Energy Reviews* 33 (May 2014), pp. 74–86. ISSN: 13640321. DOI: 10.1016/j.rser.2014.02.003.

[2] D.P. Schlachtberger et al. "The Benefits of Cooperation in a Highly Renewable European Electricity Network". en. In: *Energy* 134 (Sept. 2017), pp. 469–481. ISSN: 03605442. DOI: 10.1016/j.energy.2017.06.004.

[3] Aqeel Ahmed Bazmi and Gholamreza Zahedi. "Sustainable Energy Systems: Role of Optimization Modeling Techniques in Power Generation and Supply—A Review". en. In: *Renewable and Sustainable Energy Reviews* 15.8 (Oct. 2011), pp. 3480–3500. ISSN: 13640321. DOI: 10.1016/j.rser.2011.05.003.

[4] Sérgio Pereira, Paula Ferreira, and A.I.F. Vaz. "Generation Expansion Planning with High Share of Renewables of Variable Output". en. In: *Applied Energy* 190 (Mar. 2017), pp. 1275–1288. ISSN: 03062619. DOI: 10.1016/j.apenergy.2017.01.025.

[5] J. Bialek. "Tracing the Flow of Electricity". en. In: *IEE Proceedings - Generation, Transmission and Distribution* 143.4 (1996), p. 313. ISSN: 13502360. DOI: 10.1049/ip-gtd:19960461.

[6] F.D. Galiana, A.J. Conejo, and H.A. Gil. "Transmission Network Cost Allocation Based on Equivalent Bilateral Exchanges". en. In: *IEEE Transactions on Power Systems* 18.4 (Nov. 2003), pp. 1425–1431. ISSN: 0885-8950. DOI: 10.1109/TPWRS.2003.818689.

[7] Mohammad Shahidehpour, Hatim Yamin, and Zuyi Li. *Market Operations in Electric Power Systems*. en. New York, USA: John Wiley & Sons, Inc., Apr. 2002. ISBN: 978-0-471-44337-7 978-0-471-22412-9. DOI: 10.1002/047122412X.

[8] Yi Meng and Benjamin Jeyasurya. "Investigation of Transmission Cost Allocation Using a Power Flow Tracing Method". In: *2007 IEEE Power Engineering Society General Meeting*. Tampa, FL, USA: IEEE, June 2007, pp. 1–7. ISBN: 978-1-4244-1296-9 978-1-4244-1298-3. DOI: 10.1109/PES.2007.385565.

[9] Bo Tranberg et al. "Flow-Based Analysis of Storage Usage in a Low-Carbon European Electricity Scenario". English. In: *arXiv:1806.02549 [physics]* (June 2018). arXiv: 1806.02549 [physics].

[10] Javad Nikoukar and Mahmoud Reza Haghifam. "Transmission Pricing and Recovery of Investment Costs in the Deregulated Power System Based on Optimal Circuit Prices". en. In: *Journal of Zhejiang University SCIENCE C* 13.1 (Jan. 2012), pp. 48–57. ISSN: 1869-1951, 1869-196X. DOI: 10.1631/jzus.C1100076.

[11] Amirsaman Arabali, Seyed Hamid Hosseini, and Moein Moeini-Aghtaie. "Pricing of Transmission Services: An Efficient Analysis Based on Fixed and Variable Imposed Costs". In: *2012 11th International Conference on Environment and Electrical Engineering*. Venice, Italy: IEEE, May 2012, pp. 407–412. ISBN: 978-1-4577-1829-8 978-1-4577-1830-4 978-1-4577-1828-1. DOI: 10.1109/EEEIC.2012.6221412.

[12] T. Wu, Z. Alaywan, and A.D. Papalexopoulos. "Locational Marginal Price Calculations Using the Distributed-Slack Power-Flow Formulation". en. In: *IEEE Transactions on Power Systems* 20.2 (May 2005), pp. 1188–1190. ISSN: 0885-8950. DOI: 10.1109/TPWRS.2005.846156.

[13] ENTSO-E. "Completing the Map – Power System Needs in 2030 and 2040". en. In: (2020), p. 70.

[14] Bundesnetzagentur. *Netzentwicklungsplan Strom — Netzentwicklungsplan*. https://www.netzentwicklungsplan.de/de. 2020.

[15] Fred C. Schweppe et al. *Spot Pricing of Electricity*. en. Boston, MA: Springer US, 1988. ISBN: 978-1-4612-8950-0 978-1-4613-1683-1. DOI: 10.1007/978-1-4613-1683-1.

[16] T. Brown and L. Reichenberg. "Decreasing Market Value of Variable Renewables Is a Result of Policy, Not Variability". In: *arXiv:2002.05209 [econ, math, q-fin]* (Feb. 2020). arXiv: 2002.05209 [econ, math, q-fin].

[17] Fabian Hofmann et al. *Flow Allocation in Meshed AC-DC Electricity Grids*. en. Preprint. PHYSICAL SCIENCES, Jan. 2020. DOI: 10.20944/preprints202001.0352.v1.

[18] Jonas Hörsch et al. *PyPSA-Eur: An Open Optimisation Model of the European Transmission System (Code)*. Zenodo. June 2020. DOI: 10.5281/ZENODO.3520874.

[19] Jonas Hörsch et al. "PyPSA-Eur: An Open Optimisation Model of the European Transmission System". English. In: *Energy Strategy Reviews* 22 (Nov. 2018), pp. 207–215. ISSN: 2211467X. DOI: 10.1016/j.esr.2018.08.012.

[20] ENTSO-E. *ENTSO-E Transmission System Map*. en-us. https://www.entsoe.eu/data/map/.

[21] EEA. "Corine Land Cover (CLC) 2012, Version 18.5.1". In: (2012).

[22] EEA. "Natura 2000 Data - the European Network of Protected Sites". In: (2016).

[23] Antonio J. Conejo et al. "Z-Bus Transmission Network Cost Allocation". English. In: *IEEE Transactions on Power Systems* 22.1 (Feb. 2007), pp. 342–349. ISSN: 0885-8950. DOI: 10.1109/TPWRS.2006.889138.

[24] Thomas Schröder and Wilhelm Kuckshinrichs. "Value of Lost Load: An Efficient Economic Indicator for Power Supply Security? A Literature Review". In: *Frontiers in Energy Research* 3 (Dec. 2015). ISSN: 2296-598X. DOI: 10.3389/fenrg.2015.00055.

[25] Bundesministerium für Wirtschaft und Energie. *Verbundvorhaben: NET-ALLOK - Methoden Und Anwendungen Der Netzkostenallokation, Teilvorhaben: Methoden Und Analyse von Kostenallokationsmethoden Im Betrieb Des Elektrizitätssystems*. https://www.enargus.de/pub/bscw.cgi/?op=enargus.eps2&v=10&s=14&q=EA3310&id=399670&p=10.

[26] Chira Achayuthakan et al. "Electricity Tracing in Systems With and Without Circulating Flows: Physical Insights and Mathematical Proofs". en. In: *IEEE Transactions on Power Systems* 25.2 (May 2010), pp. 1078–1087. ISSN: 0885-8950, 1558-0679. DOI: 10.1109/TPWRS.2009.2037506.